The Mini-EUSO telescope on board the International Space Station: mission results in view of UHECR measurements from space

M. Bertaina,[a,b,*] **M. Abrate,**[a,b] **D. Barghini,**[b,c] **M. Battisti,**[d] **A. Belov,**[e,f]

M. Bianciotto,[a,b] **F. Bisconti,**[g] **C. Blaksley,**[h] **S. Blin,**[i] **F. Capel,**[j] **M. Casolino,**[d,g,h]

I. Churilo,[k] **M. Crisconio,**[l] **C. De La Taille,**[m] **T. Ebisuzaki,**[h] **F. Fenu,**[l] **M.A. Franceschi,**[n]

C. Fuglesang,[o] **A. Golzio,**[b,p] **P. Gorodetzky,**[i] **F. Kajino,**[q] **H. Kasuga,**[h] **P. Klimov,**[e]

V. Kuznetsov,[k] **M. Manfrin,**[a,b] **A. Marcelli,**[g] **L. Marcelli,**[d] **W. Marszał,**[r] **G. Mascetti,**[l]

M. Mignone,[b] **H. Miyamoto,**[a,b] **A. Murashov,**[f] **T. Napolitano,**[n] **H. Ohmori,**[h] **E. Parizot,**[i]

P. Picozza,[d,g] **L.W. Piotrowski,**[s] **Z. Plebaniak,**[d,g] **G. Prévôt,**[i] **E. Reali,**[d,g] **F. Reynaud,**[a,b]

M. Ricci,[d,n] **G. Romoli,**[d,g] **S. Sharakin,**[f] **K. Shinozaki,**[r] **J. Szabelski,**[t] **Y. Takizawa,**[h]

G. Valentini,[l] **M. Vrabel,**[r] **M. Zotov**[f] **and the JEM-EUSO Collaboration**

[a]*Department of Physics, University of Turin, V. P. Giuria 1, 10125 Turin, Italy*

[b]*INFN Section of Turin, Via P. Giuria 1, 10125 Turin, Italy*

[c]*INAF Astrophysics Observatory of Turin, Via Osservatorio 20, 10025 Pino Torinese, Italy*

[d]*INFN Section of Rome Tor Vergata, Via della Ricerca Scientifica 1, 00133 Rome, Italy*

[e]*Faculty of Physics, M.V. Lomonosov Moscow State University, ul. Kolmogorova 1(2), 119234 Moscow, Russia*

[f]*Skobeltsyn Institute of Nuclear Physics, Lomonosov Moscow State Univ., ul. Kolmogorova 1(2), 119991 Moscow, Russia*

[g]*Department of Physics, University of Rome Tor Vergata, Via della Ricerca Scientifica 1, 00133 Rome, Italy*

[h]*RIKEN, 2-1 Hirosawa Wako, Saitama 351-0198, Japan*

[i]*APC, Universitè Paris Citè, CNRS, Astroparticule et Cosmologie, 10 Rue Alice Domon et Léonie Duquet, 75013 Paris, France*

[j]*Technical University of Munich, Arcisstraße 21, 80333 Munich, Germany*

[k]*S.P. Korolev Rocket and Space Corporation Energia, Lenin str., 4a Korolev, 141070 Moscow area, Russia*

[l]*ASI, Italian Space Agency, Via del Politecnico, 00133 Rome, Italy*

[m]*Omega, Ecole Polytechnique, CNRS/IN2P3, Rte de Saclay, 91120 Palaiseau, France*

[n]*INFN National Laboratories of Frascati, Via Enrico Fermi 54, 00044 Frascati, Italy*

[o]*KTH Royal Institute of Technology, Brinellvägen 8, 114 28 Stockholm, Sweden*

[p]*Arpa Piemonte, via Pio VII, 9, Turin 10135, Italy*

[q]*Department of Physics, Konan University, 8 Chome-9-1 Okamoto, Higashinada Ward Kobe, Hyogo 658-8501, Japan*

[r]*National Centre for Nuclear Research, Andrzeja Sołtana 7, 05-400 Otwock, Poland*

[s]*Faculty of Physics, University of Warsaw, Ludwika Pasteura 5, 02-093 Warsaw, Poland*

[t]*Stefan Batory Academy of Applied Sciences, Stefana Batorego 64C, 96-100 Skierniewice, Poland*

E-mail: bertaina@to.infn.it

[*]Speaker

Mini–EUSO (Multiwavelength Imaging New Instrument for the Extreme Universe Space Observatory, known as *UV atmosphere* in the Russian Space Program) is the first detector of the JEM-EUSO program to observe the Earth from the International Space Station (ISS) and to validate from there the observational principle of a space-based detector for UHECR measurements. Mini-EUSO is a telescope operating in the near UV range, mainly between 290 – 430 nm, with a square Focal Surface (FS) corresponding to a Field of View (FoV) of ∼ 44°. Its spatial resolution at ground level is ∼ 6.3 km. Mini-EUSO was launched with the uncrewed Soyuz MS-14. The first observations, from the nadir-facing UV transparent window in the Russian Zvezda module, took place on October 7, 2019. The detector size ($37 \times 37 \times 62$ cm^3) was mainly constrained by the window size. The detector is usually installed during onboard night-time a couple of times per month, approximately at 18:30 UTC with operations lasting about 12 hours. So far, 139 sessions of data acquisition have been performed. Data are stored locally on USB solid state disks. After each data-taking session ∼10% of stored data, usually corresponding to the beginning and the end of each session, are copied and transmitted to ground to verify the correct functioning of the instrument. Till now, the data of the first full 44 sessions returned to Earth and is being analysed. The Mini–EUSO FS, or Photon Detector Module (PDM), consists of a square matrix of 36 Multi-Anode Photomultiplier Tubes (MAPMTs). Each MAPMT consists of 8×8 pixels. A group of 2×2 MAPMTs forms an Elementary Cell (EC). In total there are 2304 channels. Each EC has an independent high voltage power supply (HVPS) and board connecting four MAPMTs. The HVPS system, based on a Cockroft-Walton circuit, has an internal safety mechanism which operates either reducing the collection efficiency or the gain of the MAPMTs when particularly bright signals occurr. The optics are based on two 25 cm diameter Fresnel lenses with a point spread function of 1.2 pixels. UV bandpass filters are glued in front of the MAPMTs.

The system has a single photon-counting capability with a double pulse resolution of ∼ 6 ns. Photon counts are summed in Gate Time Units (GTUs) of 2.5 μs. The PDM Data Processor stores the 2.5 μs GTU data stream (D1) in a running buffer on which runs the trigger code. Sums of 128 frames (320 μs, D2) are continuously calculated and stored in another buffer where a trigger algorithm, at this time scale, is running. Similarly, sums on 128 D2 frames (40.96 ms, D3) are calculated in real time and continuously stored. Every 5.24 s, 128 packets of D3 data, up to 4 D2 packets and up to 4 D1 packets (if triggers were present) are sent to the storage (SSDs).

Mini-EUSO measured the terrestrial UV background with unparalleled precision. The fraction of time in which the atmospheric UV light intensity allows the UHECR observation from space is ∼18%, compatible with the expectations from simulations conducted at the time of the JEM-EUSO studies. The trigger rate on spurious events remains within the requirements in nominal background conditions. It proved effective in detecting Short Light Transients (SLT), demonstrating indirectly that the JEM-EUSO technology can detect UHECRs from space as they show similarities in terms of light profile, intensity, duration and pixel pattern on the FS of Mini-EUSO, even though all these characteristics do not match at the same time for a single event and are not mistaken for real EAS-induced signals. The ability of Mini-EUSO to detect and study atmospheric phenomena like ELVES, and the ones linked to SLTs is unique and beyond the capabilities of any other atmospheric detector. That makes a space-based detector for UHECRs a unique instrument for the atmospheric science field. Mini-EUSO demonstrated to be the first experiment from space to perform a systematic study of meteor light curves and flux in a wide range of magnitudes.

1. Introduction

One of the current main goals in the field of UHECRs (Ultra-High Energy Cosmic Rays) science is to identify their astrophysical sources [1]. For this, increased statistics is one of the essential requirements. A space-based detector for UHECR research has the advantage of a very large exposure and a uniform coverage of the celestial sphere. The aim of the JEM-EUSO program [2] is to bring the study of UHECRs to space. The principle of observation is based on the detection of UV light emitted by isotropic fluorescence of atmospheric nitrogen excited by the Extensive Air Showers (EASs) in the Earth's atmosphere and forward-beamed Cherenkov radiation reflected from the Earth's surface or dense cloud tops. The JEM-EUSO program includes several missions from ground (EUSO-TA [3]), from stratospheric balloons (EUSO-Balloon [4], EUSO-SPB1 [5], EUSO-SPB2 [6], and PBR [7]), and from space (TUS [8], Mini-EUSO [9]) employing fluorescence detectors to demonstrate the feasibility of the UHECR observation from space and prepare for the large size missions such as POEMMA [10] and the currently on-hold K-EUSO [11].

2. The Mini-EUSO space telescope

A detailed description of the Mini-EUSO space telescope is reported in [9]. It has been designed to detect a photon rate per pixel from diffuse sources (nightglow, clouds, cities, etc.) in the range of values expected from a large mission in space such as the original JEM-EUSO mission [12]. The pixel FoV is, therefore, ~100 times larger in area with respect to the FoV of a JEM-EUSO pixel (0.5 km × 0.5 km), to compensate for the optical system ~100 times smaller, constrained by the dimension of the UV transparent window where Mini-EUSO is installed during the data taking sessions. As a consequence, the energy threshold of Mini-EUSO for UHECRs is well above 10^{21} eV, roughly 2 orders of magnitude higher than the original JEM-EUSO one (see Fig. 1).
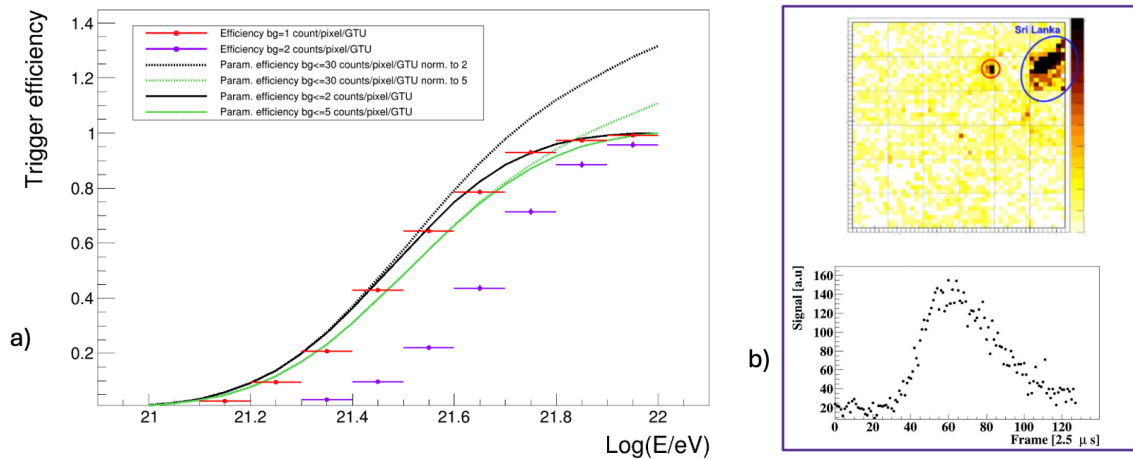

Figure 1: a) The figure shows the trigger efficiency of Mini-EUSO as a function of energy for different background conditions. See discussion on duty cycle in Sect. 3 for details. b) Image (top) and light profile (down) of a SLT detected by Mini-EUSO near Sri Lanka. The event has duration and light intensity similar to what is expected from an EAS signal even though their kinematics do not match (see discussion on Sect. 3).

Events with a duration of tens of μs, such as UHECRs, are searched with a trigger algorithm that works at the level of D1 GTUs. The algorithm searches for a signal above 16 standard deviations from the average in any pixel of the FS. In case of a trigger, the 128 frame buffer centered around the triggering GTU is stored in memory. A similar algorithm runs on D2 data to search for events with a duration of a few ms. A more detailed description of the trigger algorithm is reported in [13], which represents an adaptation of the logic conceived for JEM-EUSO [14], while the on-board performance of the trigger system is summarized in [15].

Mini-EUSO monitors the atmosphere and studies the nature, extension and duration of the transient lights, to investigate the capability of detecting light signals from EASs and minimize the rate of spurious events. Thanks to its large FoV, Mini-EUSO also acts as an atmospheric monitoring detector, observing different natural or anthropogenic phenomena ranging from the UV emission of clouds (D3 data), lightning and thunderstorm activity and study of Transient Lumoinous Events (TLEs, D1 and D2 data), in particular ELVES, up to much slower events (D3 data) like meteors [16], nuclearites [17] or space debris [18] with a sensitivity to fainter events beyond the usual capabilities of atmospheric monitoring detectors, thanks to the dimension of its optical system.

Prior to the launch, the instrument underwent a series of integration and acceptance tests in Rome, Moscow, and Baikonur cosmodrome, where it was enclosed in the uncrewed Soyuz capsule. A systematic test of the acquisition logic was performed at the TurLab facility [19] (Univ. of Turin) and at the Astrophysical Observatory of Turin (INAF-OATo) [20]. After launch, an end-to-end in-flight calibration of the detector has been performed by assembling different UV-flasher systems on ground in Japan, Italy, and France and by firing them in various observational campaigns [21]. It made use of a flasher system consisting of an array of 9 100W COB-UV LEDs, batteries and an Arduino circuit. This system was absolutely calibrated at APC (Univ. Paris Cité) and at the TurLab facility. In October 2022, an observational campaign was performed at Sant'Antimo Abbey (Italy) at the altitude of ~320 m a.s.l. The place was chosen based on the very low light pollution in an area of several km radius. Photons from the UV flasher were detected and the overall efficiency of Mini-EUSO telescope was estimated to be $\epsilon_{ME} = 0.061 \pm 0.020$ at $\lambda = 397$ nm.

3. Duty cycle and exposure

Fig. 2 shows a portion of Mini-EUSO orbit on Session 30, which took place on January 9th 2021 around 7:30 UTC. It displays an example of the different conditions that Mini-EUSO observes during an orbit: clear sky, cloudy conditions, city lights and land. Image a) shows the UV map as a function of longitude and latitude. The counts/pix/GTU are color coded in image b). They have been taken in D3 mode but normalized to the D1 GTU. Plot c) displays the light curve along the orbit of one pixel of Mini-EUSO. Plot d) presents the map of artificial lights in US and Canada [22] where the intensity is expressed in fractions above natural light intensity, while e) the atmospheric conditions during the passage over ocean by means of a post-processing analysis of the weather forecast obtained with the data collected by the Global Forecast System (GFS) [23]. The orbit of Mini-EUSO is highlighted by the three lines indicating the center and edges of the FoV of Mini-EUSO. As expected the lowest counts are detected over ocean on clear atmospheric conditions. In the presence of clouds the counts increase and the color contour matches in general the shape of the cloud location. The city lights of Hawaii islands are clearly visible in both a) (yellow spot) and

c) (sharp peak increase of light). The presence of thunderstorm activity in the cloudy area between 7h36 and 7h39 UTC can be deduced by the pixel data reported in c) which show rapid increase and decrease of photon counts. Before entering the US coast there is a less cloudy region and the counts tend to decrease. Afterwards, when entering the US west coast sudden peaks in photon counts are observed. They are due to the passage on particularly bright areas as depicted in map d). The counts remain higher than over the ocean also in the much less urbanized areas of Canada. This is due to the presence of snow which is highly reflective. The slightly higher counts on the St. Lawrence Bay in Quebec are due to the presence of low clouds. When Mini-EUSO goes back over the ocean the light intensity decreases again to ocean levels. The final sudden increase of counts is due to the sunrise which ends the night time of the orbit. This example shows the capability of the UV camera of Mini-EUSO to infer autonomously different atmospheric or ground scenarios encountered during the flight. Mini-EUSO results on the average UV emissions in different conditions: clear and cloudy
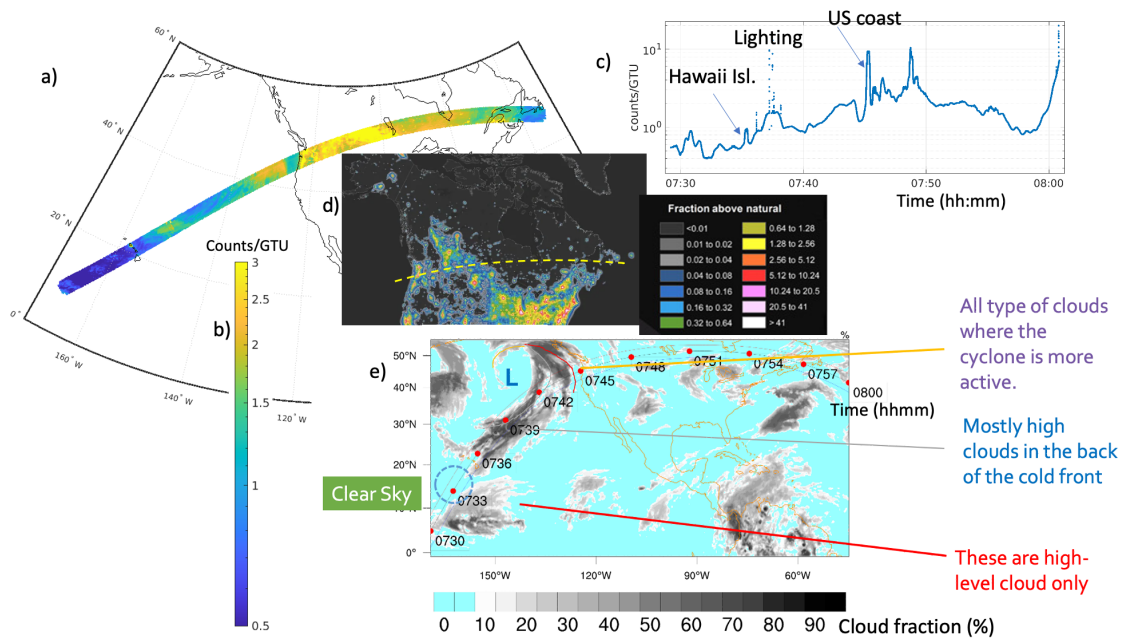

Figure 2: The figure shows a portion of an orbit of Mini-EUSO on Session 30 (January 9th 2021). Image a) shows the UV map of Mini-EUSO as a function of longitude and latitude. The counts/pix/GTU are color-coded in image b). They have been taken in D3 mode but normalized to the D1 GTU. Plot c) displays the light curve along the orbit of one pixel of Mini-EUSO. Plot d) presents the map of artificial lights taken from [22] (with a scale in fraction above natural light intensity), while e) the atmospheric conditions during the passage over ocean by means of a GFS post-processing analysis of the weather forecasts. The orbit of Mini-EUSO is highlighted by the three lines indicating the center and edges of the FoV. See text for details.

conditions, sea and land, various lunar phases are reported in [24]. Assuming no-moon conditions and typical land/ocean and clear/cloudy atmosphere ratios equal to 30/70, the average background level is ~1.3 counts/pix/GTU, slightly below 1 counts/pix/GTU on ocean and clear sky, while a factor 1.5 - 2 higher in presence of clouds. The average counts on land are ~1.5 times higher than on ocean due to the tail of the distribution associated to the passage over civilized areas. However, deserts and forests have much lower background values, ideal for collecting low energy events.

Fig. 1a) shows the trigger efficiency curves of Mini-EUSO as a function of energy for different background conditions obtained using ESAF simulated proton EASs [25]. The curves are obtained either with fixed background conditions of 1 or 2 counts/pix/GTU, or as cumulative distributions. In this second case the cumulative trigger efficiency curve is determined as a weighted sum of each trigger efficiency curve obtained for a specific background level and for the fraction of time in which it occurred. The weighted sum stops at 2 or 5 counts/pix/GTU or extends till 30 counts. The fraction of time in which the measured background by Mini-EUSO is less than 2(5) counts corresponds to a duty cycle of ~15%(18%). The range of sessions between 20 and 44 have been used to perform this calculation which corresponds to the period in which Mini-EUSO operated in nominal conditions. The fact that both black and green curves tightly enclose the red points obtained at the fixed background level of 1 count/pix/GTU, which was assumed in the pre-flight simulations, confirms the derived duty cycle. This value is very similar to what was considered in the simulations of JEM-EUSO exposure [26]. The effect of clouds is not included yet. In JEM-EUSO a cloud efficiency of k_c = 0.72 was estimated. More details on the methodology to derive Mini-EUSO exposure curves and to determine the duty cycle can be found in [27].

The geometrical aperture of Mini-EUSO is obtained by multiplying the footprint of each pixel for 2304 available pixels. Considering the solid angle and the same cloud efficiency k_c of JEM-EUSO, the collected exposure in these 25 sessions corresponds to 1200 Linsley at energies with full efficiency. The projected exposure considering all the data sessions from number 20 to 139 gives a value of ~6000 Linsley. This value is comparable to the one accumulated by ground experiments with hybrid data. Finally, an extrapolation, in the case of continuous operation of Mini-EUSO during the past 5 years, leads to a potentially accumulated exposure at the highest energies of ~150,000 Linsley, which is comparable with that collected so far by the surface detectors of the ground-based experiments. These results, despite being obtained with simplified assumptions, provide a good idea of the potential of a space-based observatory devoted to the study of UHECRs.

The D1 trigger logic aims at detecting short pulses with time scales comparable to EASs. The most interesting categories of most frequent detected events are Ground Flashers (GFs) and SLTs. They are both identified by visually searching for short pulses which are either repeated or not. Sometimes they trigger two consecutive packets and the full shape is visible. Those with a duration ≤ 200 μs were looked at more carefully to check their compatibility with EAS-like events. The visual inspection of the events identified 561 different GFs, some of which with comparable light intensity or event duration of EASs. However, their periodic repetition and a careful comparison with EAS profiles and images on the FS allowed to discriminate them. The same inspection identified 14 SLTs (one of them is shown in Fig. 1b). The origin of those fast flashing lights is still under study, but it seems safe to assume that at least some of them are linked to the thunderstorm activity in the atmosphere. None of them could be misunderstood with an EAS (details in [28]).

4. Atmospheric Phenomena

Mini-EUSO spatial resolution of $\simeq$ 4.7 km at the ionospheric level, combined with a temporal resolution of 2.5 μs, has proven to be well suited for the detection of ELVES, which are transient flashes of light expanding radially in the lower ionosphere (75 - 105 km altitude), as rings of increasing radius. Mini-EUSO detected 37 ELVES so far. They are traced in their horizontally

expanding, fast ring-shaped light emission. ELVES appear as bright arcs of light on the telescope's FS, expanding over time. In general, several D1 GTUs are associated with each event, having ELVES a duration of hundreds of μs. The typical total duration of the detected events reaches a maximum of ~0.5 ms, consistent with results reported in the literature. The detected ELVES are located mostly in the equatorial region (see Fig. 3a). More details can be found in [29].
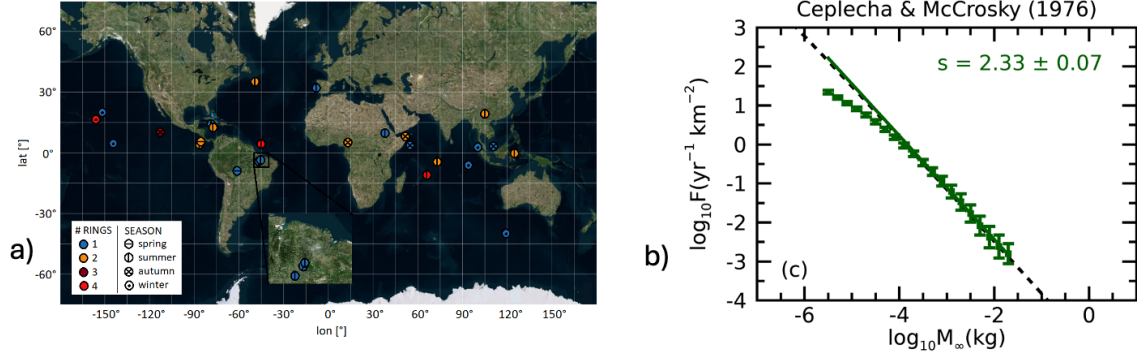

Figure 3: a) Location (latitude-longitude) of the ELVEs detected with Mini-EUSO. Most of them are distributed in the equatorial region. Three events in East Brazil occurred at an interval of 18 and 5 seconds (second from first and third from second respectively) one from the other. b) Cumulative flux density distribution of meteoroids observed by Mini-EUSO. The method described in [30] has been used to compute the pre-atmospheric mass of the meteoroid. Coloured squares plot the results of Mini-EUSO. The thick coloured line reports the result of a linear fit in the log-log space on the half interval of large masses. The fitted value of the mass index s is reported in the corresponding panel. The black dashed line plots the flux estimated from [31] for which $s = 2.34$ (see [16] for details).

Within a total observing time of 5.7 days during its first 44 operative sessions, the observations of Mini-EUSO provided an extensive database of ~24,000 meteor events up to a +6 limiting absolute magnitude, proving that space-based observations can significantly increase the statistics achievable with instruments operating on the ground. Thanks to the development of dedicated simulations to estimate the total exposure time of Mini-EUSO for the observation of meteors, it was possible to provide an estimation of the absolute flux density of meteors that was found to be comparable with other results available in the literature (see Fig. 3b).

5. Acknowledgements

References

[1] A. Coleman et al., *Astrop. Phys.* **147** (2023) 102794

[2] M. Ricci (JEM-EUSO Coll.), *J. Phys. Conf. Ser.* **718 n.5** (2016) 052034.

[3] G. Abdellaoui *et al* (JEM-EUSO Coll.), *Astrop. Phys.* **102** (2018) 98-111.

[4] J.H. Adams Jr. *et al* (JEM-EUSO Coll.), *Space Sci. Rev.* **218** (2022) 3.

[5] G. Abdellaoui *et al* (JEM-EUSO Coll.), *Astrop. Phys.* **154** (2024) 102891.

[6] J. H. Adams Jr. *et al* (JEM-EUSO Coll.), *Astrop. Phys.* **165** (2025) 103046.

[7] M. Battisti *et al* (JEM-EUSO Coll.), *Nucl. Instr. & Meth. A* **1068** (2024) 169727.

[8] P. Klimov *et al* (TUS Coll.), *Space Sci. Rev.* **212** (2017) 1687-1703.

[9] S. Bacholle *et al*, *ApJS* **253** (2021) 36.

[10] A. Olinto *et al* (POEMMA Coll.), *JCAP* **06** (2021) 007.

[11] P. Klimov *et al* (JEM-EUSO Coll.), *Universe* **8** (2022) 88.

[12] J.H. Adams Jr. *et al.* (JEM-EUSO Coll.), *Astrop. Phys.* **44** (2013) 76-90.

[13] A. Belov *et al.* (JEM-EUSO Coll.), *ASR* **62/10** (2018) 2966-2976.

[14] G. Abdellauoi *et al.* (JEM-EUSO Coll.), *NIMA* **866** (2017) 150-163.

[15] M. Battisti *al.* (JEM-EUSO Coll.), *ASR* **70/9** (2022) 2750-2766.

[16] D. Barghini *et al.* (JEM-EUSO Coll.), *Astr. & Astr.* **687** (2024) A304.

[17] J.H. Adams *et al.* (JEM-EUSO Coll.), *Exp. Astr.* **40** (2015) 253-279.

[18] L. Olivi *et al.* (JEM-EUSO Coll.), *IEEE JSTARS* **17** (2024) 10432 - 10453.

[19] P. Barrillon *et al.* (JEM-EUSO Coll.), *Exp. Astr.* **55/2** (2023) 569 - 602.

[20] F. Bisconti *et al.* (JEM-EUSO Coll.), *Exp. Astr.* **53/1** (2021) 133-158.

[21] M. Battisti *et al.* (JEM-EUSO Coll.), *Astrop. Phys.* **165**(2025) 103057.

[22] F. Falchi *et al.*, *Science Advances* **2/6** (2016) 062005.

[23] Nat. Cent. for Environ. Pred., Nat. Weather Serv., NOAA, U.S. Dep. of Comm., (2007).

[24] D. Barghini *et al.* (JEM-EUSO Coll.), *Rem.Sens.Env.* **284** (2023) 113336.

[25] S. Abe *et al.* (JEM-EUSO Coll.), *Eur.Phys.J.C* **83** (2023) 1028.

[26] J. H. Adams Jr. *et al.* (JEM-EUSO Coll.), *Astrop. Phys.* **44** (2013) 76 - 90.

[27] M. Bertaina *et al.* (JEM-EUSO Coll.), *EPJ Web of Conf.* **283** (2023) 06008.

[28] M. Battisti *et al.* (JEM-EUSO Coll.), *PoS(ICRC2023)* **444** (2023) 353.

[29] G. Romoli *et al.* (JEM-EUSO Coll.), *PoS(ICRC2023)* **444** (2023) 223.

[30] Z. Ceplecha and R. E. McCrosky, *J. Geop. Res.* **81** (1976) 6257 - 6275.

[31] E. Grun *et al.*, *Icarus* **62** (1985) 244 - 272.